

## Anomalously low solar extreme-ultraviolet irradiance and thermospheric density during solar minimum

Stanley C. Solomon,<sup>1</sup> Thomas N. Woods,<sup>2</sup> Leonid V. Didkovsky,<sup>3</sup> John T. Emmert,<sup>4</sup> and Liying Qian<sup>1</sup>

Received 23 June 2010; accepted 1 July 2010; published 25 August 2010.

[1] Solar activity during 2007–2009 was very low, and during this protracted solar minimum period, the terrestrial thermosphere was cooler and lower in density than expected. Measurements from instruments on the SOHO and TIMED spacecraft, and by suborbital rocket flights, indicate that solar extreme-ultraviolet irradiance levels were lower than they were during the previous solar minimum. Analysis of atmospheric drag on satellite orbits indicate that the thermosphere was lower in density, and therefore cooler, and than at any time since the beginning of the space age. However, secular change due to increasing levels of carbon dioxide and other greenhouse gases, which cool the upper atmosphere, also plays a role in thermospheric climate. Simulations by the NCAR Thermosphere-Ionosphere-Electrodynamics General Circulation Model are compared to thermospheric density measurements, yielding evidence that the primary cause of the low thermospheric density was the unusually low level of solar extreme-ultraviolet irradiance. **Citation:** Solomon, S. C., T. N. Woods, L. V. Didkovsky, J. T. Emmert, and L. Qian (2010), Anomalously low solar extreme-ultraviolet irradiance and thermospheric density during solar minimum, *Geophys. Res. Lett.*, 37, L16103, doi:10.1029/2010GL044468.

### 1. Introduction

[2] Solar ultraviolet irradiance varies on periods associated with the 11-year solar cycle and the 27-day solar rotational period. This variation increases with decreasing wavelength, reaching factors of two to ten in the extreme ultraviolet (EUV) (10–120 nm). EUV photons are absorbed in the Earth's thermosphere, the atmospheric region between ~90 and ~500 km, creating the ionosphere within it, and causing its temperature to increase with altitude, reaching ~600 K at 400 km (at solar minimum) and as high as ~1500 K (at solar maximum). This large, cyclical temperature change causes an even larger density variation in the upper thermosphere, an order of magnitude near 400 km altitude, with increased temperature causing increased density. Quantifying these density variations with empirical and theoretical methods is important for prediction of satellite orbits, since they are

influenced by atmospheric drag, particularly during high solar activity or geomagnetic storms. Conversely, analysis of the time evolution of satellite orbital elements provides a means by which the variation of thermospheric density can be measured, and has provided much of the data upon which empirical thermospheric models are based.

[3] Superimposed on this solar-driven variation is a gradual decrease in temperature and density caused by increasing anthropogenic CO<sub>2</sub>. Roble and Dickinson [1989] predicted that a consequence of increasing CO<sub>2</sub> levels would be to decrease the temperature of the upper atmosphere, opposite to the response of the lower atmosphere, due to radiational cooling by CO<sub>2</sub>. The observed rate of change of density at a reference altitude of 400 km is estimated to be 2% to 5% per decade [Keating *et al.*, 2000; Emmert *et al.*, 2004, 2008; Marcos *et al.*, 2005], in approximate agreement with model predictions [Roble and Dickinson, 1989; Rishbeth and Roble, 1992; Akmaev and Fomichev, 2000; Qian *et al.*, 2006]. In order to avoid the complicating effects of the solar cycle, initial findings compared densities at successive solar minima. This could provide a credible methodology for assessing anthropogenic global change in the thermosphere, assuming that solar EUV returns to similar levels at each minimum. Changes in the ionosphere accompany the neutral atmosphere layers, including reduction in the height of ionospheric layers.

[4] The descending phase of solar cycle 23 was long and gradual, and during 2008–2009, solar activity became extremely low, giving rise to speculation concerning prolonged low solar activity levels such as existed during the “Maunder Minimum” (1640–1700) [Eddy, 1976]. In late 2009, solar activity finally started to increase, but the quiescent period between mid-2007 and mid-2009 was one of the longest of recent solar minima. Space-based measurements indicate that the solar EUV irradiance was also anomalously low during this time, or at least lower than the previous solar minimum. Ionospheric observations [Heelis *et al.*, 2009] find that the ionosphere was lower and cooler than typical solar minimum conditions, and results from analyses of satellite orbital elements [Emmert *et al.*, 2010] show that the upper thermosphere was significantly less dense, i.e., cooler, than the previous several solar minima, and indeed cooler than any other such period on record since the beginning of space flight. The purpose of this paper is to demonstrate through model simulations that the solar and terrestrial observations are compatible, and mutually supporting.

### 2. Solar Extreme-Ultraviolet Irradiance

[5] Evidence concerning solar EUV levels comes from several space-flight instruments, including the Solar EUV

<sup>1</sup>High Altitude Observatory, National Center for Atmospheric Research, Boulder, Colorado, USA.

<sup>2</sup>Laboratory for Atmospheric and Space Physics, University of Colorado at Boulder, Boulder, Colorado, USA.

<sup>3</sup>Space Sciences Center, University of Southern California, Los Angeles, California, USA.

<sup>4</sup>Space Science Division, Naval Research Laboratory, Washington, D. C., USA.

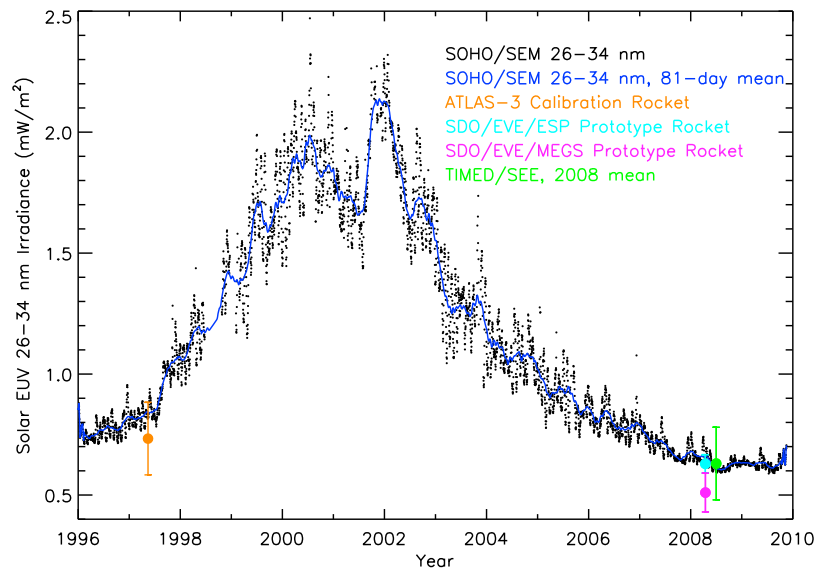


**Figure 1.** Solar EUV variation in the 26–34 nm band over solar cycle 23 measured by the SEM detector on the SOHO spacecraft. Black dots: daily average values. Blue line: 81-day centered mean (with data gaps interpolated). Estimated uncertainty is 6%. Also plotted, with estimated uncertainties, are irradiance measurements integrated over the same band from the ATLAS-3 calibration rocket on 15 May 1997 (orange), the SDO/EVE EUV SpectroPhotometer (ESP) prototype (cyan) and the SDO/EVE Multiple EUV Grating Spectrograph (MEGS) prototype (magenta) on a rocket on 14 April 2008, and the TIMED/SEE 2008 annual average (green). The decrease in SEM irradiance from 1996 to 2008 is ~15%.

Monitor (SEM) [Judge *et al.*, 1998] on the Solar and Heliospheric Observatory (SOHO), the Solar EUV Experiment (SEE) [Woods *et al.*, 2005] on the Thermosphere-Ionosphere-Mesosphere Energetics and Dynamics (TIMED) satellite, and several sub-orbital rocket flights used to calibrate these instruments. SEM has made measurements spanning the two most recent solar minima of the integrated solar EUV flux in the 26–34 nm band, which contains the bright He II line at 30.4 nm and several important coronal lines, comprising about a quarter of the total solar EUV energy flux. The SEM results from 1996 to 2010 are shown in Figure 1. These

data have been calibrated with similar instruments on eight suborbital rocket flights, and have a 6% estimated uncertainty. A reduction of 15% in solar flux measured within this wavelength band from the minimum of solar cycles 22/23 in 1996 to the minimum of solar cycles 23/24 in 2008–2009 is estimated [Didkovsky *et al.*, 2010]. Also shown on this plot are measurements during the two solar minima by different instruments integrated over the same wavelength band, including two rocket flights [Woods *et al.*, 1998, 2009; Chamberlin *et al.*, 2009], and the average of SEE daily measurements during 2008. The absolute uncertainty esti-

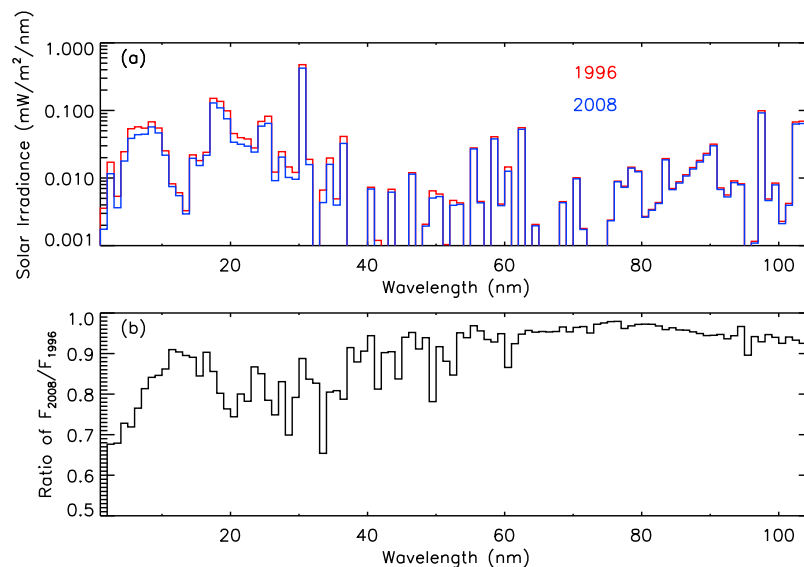


**Figure 2.** (a) Estimated solar EUV spectra at 1 nm resolution, for 1996 (red) and 2008 (blue) at the minima between solar cycle 22/23 and solar cycle 23/24, respectively. (b) Ratio of the 2008 spectrum to the 1996 spectrum.

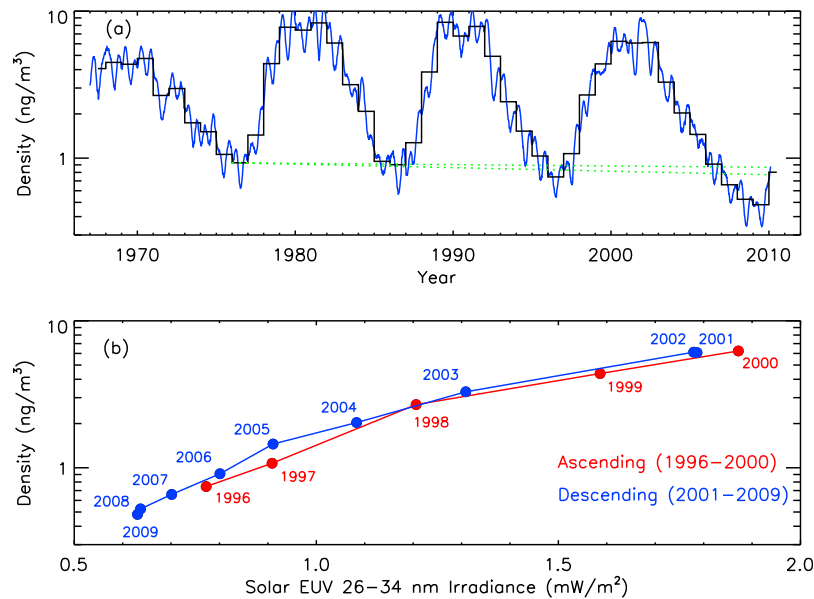


**Figure 3.** (a) Global mean thermospheric density at 400 km altitude, obtained from satellite orbital parameters over four solar cycles. Blue: 81-day centered running mean. Black: annual average. Green dotted lines: envelope of expected decrease due to increasing CO<sub>2</sub> levels, in the range of 2% to 5% per decade, starting with the 1976 annual average (see text). (b) Global mean thermospheric density annual average plotted as a function of the 26–34 nm solar EUV irradiance annual average measured by the SEM for the ascending (red) and descending (blue) phases of solar cycle 23.

mates for these measurements (~20%) are significant, but overlap the SEM measurements, and independently confirm the decrease.

[6] In order to estimate the wavelength dependence of this change, the CHIANTI models [Dere *et al.*, 1997; Landi *et al.*, 2006] of the quiet sun (QS) and coronal hole (CH) differential emission measures (DEMs) were employed. A. 50 CH proportion fit the SEM 26–34 nm average measurement for 1996, and a. 68 CH proportion fit the SEM 26–34 nm average measurement for 2008. These DEM percentages are not absolute values for the area covered on the solar disk, but are used as a basis for relative comparison. The overall reduction in EUV energy is 13%. The wavelength-dependent ratios inferred from this analysis are then applied to a solar minimum reference spectrum derived from the EUVAC solar EUV irradiance model [Richards *et al.*, 1994] at 1 nm resolution, resulting in the spectra shown in Figure 2. This model is employed as a baseline because it is the standard input to the thermospheric simulations described below.

### 3. Thermospheric Density

[7] Global-average thermospheric total mass density is derived from the effect of atmospheric drag on ~5000 objects orbiting the Earth [Emmert *et al.*, 2008, 2010; Emmert, 2009]. Solar EUV irradiance is the most important parameter affecting thermospheric density, but short-term perturbations from geomagnetic activity, and periodic seasonal variation due to changes in Sun-Earth distance and atmospheric circulation, also play a role [cf. Qian *et al.*, 2009]. These may be removed using empirical reference models in order to focus on the solar effect, as done by Emmert *et al.* [2010], but in the analysis shown here, unadjusted mass densities are employed. Figure 3a plots the 81-day centered

running mean thermospheric density at 400 km since 1966. The overall uncertainty and long-term stability are estimated at 10% and 3%, respectively. The systematic seasonal variation is apparent in this time series, so annual averages are also plotted, showing that 2007, 2008, and 2009 were the three lowest-density years on record, and that 2008–2009 were 29% lower than the solar cycle 22/23 minimum in 1996. The slight decline in each successive minimum, expected from increasing CO<sub>2</sub> levels, is also plotted, for the 2% to 5% range estimated from model and observational studies (see above). The solar cycles 23/24 minimum is well below that trend. Figure 3b compares annual averages of density to annual averages of the SEM 26–34 nm solar EUV irradiance during the ascending and descending phases of the solar cycle. Except for 2005, which may have been anomalous due to periodic geomagnetic disturbances [e.g., Lei *et al.*, 2008], the long-term correspondence is good. Density returns in 2006 to a level consistent with the 1996–1997 trend, although about 5% higher, rather than slightly lower, as would be expected from the anthropogenic CO<sub>2</sub> effects. This implies that there might be a small drift in the solar measurement that could account for 5–10% of the difference, which is within the range of the estimated uncertainties.

### 4. Model Simulations

[8] Model simulations were performed to investigate whether the estimated changes in solar EUV and CO<sub>2</sub> from 1996 to 2008 are compatible with the differences in thermospheric density, using the NCAR Thermosphere-Ionosphere-Electrodynamics General Circulation Model (TIE-GCM) v. 1.92, a numerical general circulation model of the coupled thermosphere/ionosphere system from ~97 to ~600 km altitude [Roble *et al.*, 1988; Richmond *et al.*, 1992]. The solar

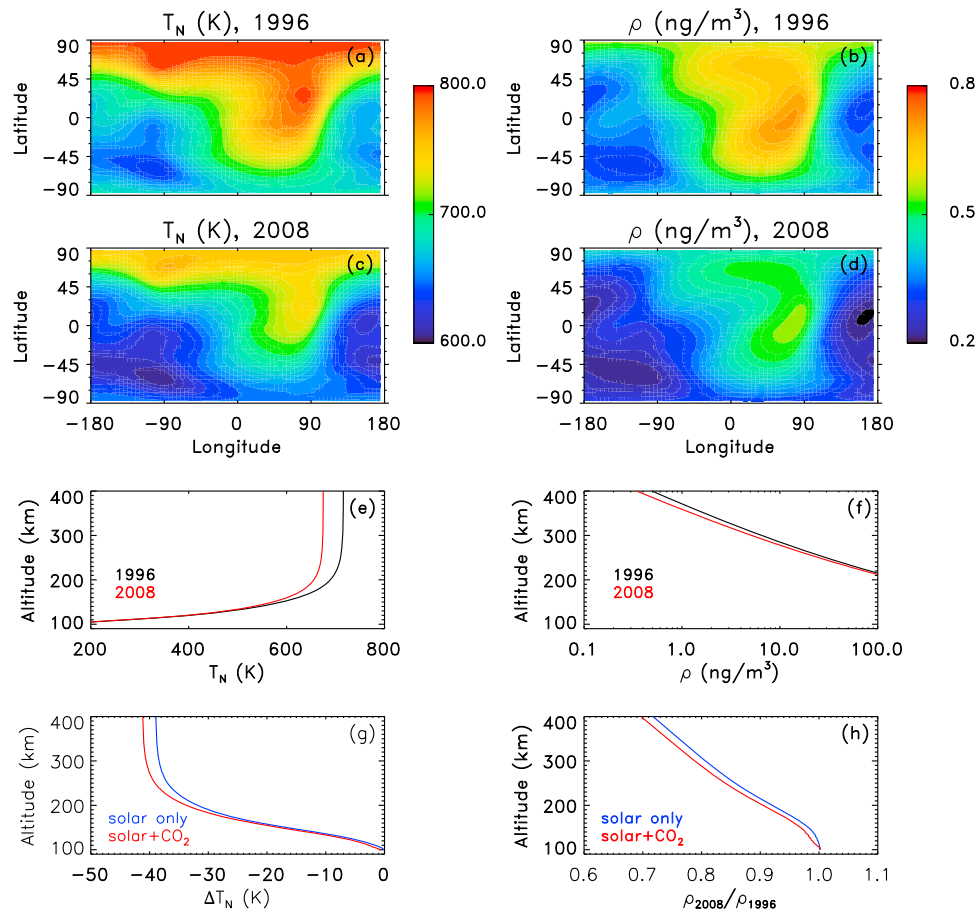


**Figure 4.** Thermospheric temperature and density modeled by the NCAR TIE-GCM on day-of-year 227 using the spectra shown in Figure 2. (a, b) Model temperature and density at 400 km for 1996. (c, d) Model temperature and density for 2008. (e, f) Global average temperature and density as a function of altitude for 1996 and 2008. Black line: 1996. Red line: 2008 with both decreased solar EUV and increased CO<sub>2</sub>. (g, h) Global average temperature change from 1996 to 2008, and density ratio for 2008 divided by 1996, as a function of altitude. Black line: 1996. Blue line: 2008 with only solar EUV decrease. Red line: 2008 with both decreased solar EUV and increased CO<sub>2</sub>.

input was derived from the 1-nm resolution spectra shown in Figure 2 for 1996 and 2008 using the method of *Solomon and Qian* [2005]. Constant low geomagnetic forcing ( $K_p = 1$ ) was assumed throughout the simulation period. The semi-annual and annual density periodicities were obtained by specifying seasonal variation of the eddy diffusivity coefficient at the lower boundary [*Qian et al.*, 2009]. The CO<sub>2</sub> mixing ratio imposed at the lower boundary was 360 ppmv for 1996 and 385 ppmv for 2008. The model was run for an 81-day period (day-of-year 150 to 230) for three cases: 1996 solar input, 2008 solar input with CO<sub>2</sub> unchanged, and 2008 solar input with increased CO<sub>2</sub>.

[9] Figure 4 shows the results of these simulations for day-of-year 227, typical of any day within the model period. The left column displays temperature and the right column displays density, both at the reference altitude of 400 km. The color contour plots specify the global distribution of temperature and density for the 1996 and for the combined 2008 runs. The line plots give the global average altitude dependence of the changes, and show the effect of including (red line) and neglecting (blue line) the CO<sub>2</sub> change. The change due to increased CO<sub>2</sub> levels is much smaller than the change due to solar EUV. The combined decrease in temperature is 41 K, ~2 K of which is attributable to CO<sub>2</sub>

increase, and the combined decrease in density is 31%, ~3% of which is attributable to CO<sub>2</sub> increase. The model densities are in good agreement with global average densities shown in Figure 3 for 1996 and 2008, and the density decrease is very close to the 29% inter-minima difference derived from satellite drag measurements.

## 5. Conclusions

[10] Due to the difficulty of calibrating long-term space-based measurements of solar EUV, evidence from those measurements taken alone is compelling but not definitive. Although solar EUV is the primary controller of the temperature and density of the thermosphere, contributions from geomagnetic activity, and changes in atmospheric circulation and composition, are also significant. However, it is unlikely that three successive years of record-low densities could occur due to these effects. Estimates of anthropogenic forcing suggest that it can only account for a small portion of the observed density change. Therefore, the thermosphere provides evidence supporting the assertion that solar EUV was lower than it was during preceding solar minima. The wavelength spectrum of this change is not well known, but the thermospheric global mean temperature and density are

insensitive to details of the solar spectrum because they respond to integrated EUV energy. Model simulations show that the estimated change in total EUV energy input employed here is approximately commensurate with the measured density change.

[11] A remaining challenge is to explain why the Sun is different, and to what extent other regions of the solar spectrum might be affected. Solar EUV images indicate lower radiance from areas of “open” solar magnetic field known as coronal holes. Low-latitude coronal holes were particularly prevalent during the declining phase of solar cycle 23 and the minimum of cycle 23/24, which could offer an explanation for the lower EUV irradiance. In addition to the effects of large-scale coronal holes, it is possible that the long-term lack of new magnetic flux emerging in the solar photosphere results in a higher proportion of “open” field lines, and hence a predominantly cooler and darker corona, on smaller scales than detectable by full-disk EUV imagers.

[12] Speculation that the Sun might be entering a new “Maunder Minimum,” turned out to be unfounded, but it is possible that the extended intercycle minimum period has given us a glimpse what it might have been like. Future investigation of upper atmosphere climate change will be complicated by the fact that the concept of a “typical” solar minimum is no longer tenable.

[13] **Acknowledgments.** This research was supported by NASA grant NNH10AN621 and ONR funding to the Naval Research Laboratory, NASA grant NAG5-11408 to the University of Colorado, NASA grant NNX08AM74G to the University of Southern California, and NASA grants NNX10AF21G and NNX07AC61G to the National Center for Atmospheric Research. NCAR is supported by the National Science Foundation.

## References

- Akmaev, R. A., and V. I. Fomichev (2000), A model estimate of cooling in the mesosphere and lower thermosphere due to the CO<sub>2</sub> increase over the last 3–4 decades, *Geophys. Res. Lett.*, *27*, 2113, doi:10.1029/1999GL011333.
- Chamberlin, P. C., T. N. Woods, D. A. Crotser, F. G. Eparvier, R. A. Hock, and D. L. Woodraska (2009), Solar cycle minimum measurements of the solar extreme ultraviolet spectral irradiance on 14 April 2008, *Geophys. Res. Lett.*, *36*, L05102, doi:10.1029/2008GL037145.
- Dere, K. P., E. Landi, H. E. Mason, B. C. Monsignori Fossi, and P. R. Young (1997), CHIANTI—An atomic database for emission lines, I, Wavelengths greater than 50 Å, *Astron. Astrophys.*, *125*, Suppl., 149.
- Didkovsky, L. V., D. L. Judge, and S. R. Wieman (2010), Minima of solar cycles 22/23 and 23/24 as seen in SOHO/CELIAS/SEM absolute solar EUV flux, in *SOHO-23: Understanding a Peculiar Solar Minimum*, edited by S. R. Cranmer, J. T. Hoeksema, and J. Kohl, *ASP Conf. Ser.*, *428*, 73.
- Eddy, J. A. (1976), The Maunder Minimum, *Science*, *192*, 1189, doi:10.1126/science.192.4245.1189.
- Emmert, J. T. (2009), A long-term data set of globally averaged thermospheric total mass density, *J. Geophys. Res.*, *114*, A06315, doi:10.1029/2009JA014102.
- Emmert, J. T., J. M. Picone, J. L. Lean, and S. H. Knowles (2004), Global change in the thermosphere: Compelling evidence of a secular decrease in density, *J. Geophys. Res.*, *109*, A02301, doi:10.1029/2003JA010176.
- Emmert, J. T., J. M. Picone, and R. R. Meier (2008), Thermospheric global average density trends, 1967–2007, derived from orbits of 5000 near-Earth objects, *Geophys. Res. Lett.*, *35*, L05101, doi:10.1029/2007GL032809.
- Emmert, J. T., J. L. Lean, and J. M. Picone (2010), Observations of record-low thermospheric densities during the 2008 solar minimum, *Geophys. Res. Lett.*, *37*, L12102, doi:10.1029/2010GL043671.
- Heelis, R. A., W. R. Coley, A. G. Burrell, M. R. Hairston, G. D. Earle, M. D. Perdue, R. A. Power, L. L. Harmon, B. J. Holt, and C. R. Lippincott (2009), Behavior of the O<sup>+</sup>/H<sup>+</sup> transition height during the extreme solar minimum of 2008, *Geophys. Res. Lett.*, *36*, L00C03, doi:10.1029/2009GL038652.
- Judge, D. L., et al. (1998), First solar EUV irradiances obtained from SOHO by the CELIAS/SEM, *Sol. Phys.*, *177*, 161, doi:10.1023/A:1004929011427.
- Keating, G. M., R. H. Tolson, and M. S. Bradford (2000), Evidence of long-term global decline in the Earth’s thermospheric densities apparently related to anthropogenic effects, *Geophys. Res. Lett.*, *27*, 1523, doi:10.1029/2000GL003771.
- Landi, E., G. Del Zanna, P. R. Young, K. P. Dere, H. E. Mason, and M. Landini (2006), CHIANTI—An atomic database for emission lines, VII, New data for X-rays and other improvements, *Astrophys. J.*, *162*, Suppl., 261, doi:10.1086/498148.
- Lei, J., J. P. Thayer, J. M. Forbes, E. K. Sutton, and R. S. Nerem (2008), Rotating solar coronal holes and periodic modulation of the upper atmosphere, *Geophys. Res. Lett.*, *35*, L10109, doi:10.1029/2008GL033875.
- Marcos, F. A., J. O. Wise, M. J. Kendra, N. J. Grossbard, and B. R. Bowman (2005), Detection of a long-term decrease in thermospheric neutral density, *Geophys. Res. Lett.*, *32*, L04103, doi:10.1029/2004GL021269.
- Qian, L., R. G. Roble, S. C. Solomon, and T. J. Kane (2006), Calculated and observed climate change in the thermosphere, and a prediction for solar cycle 24, *Geophys. Res. Lett.*, *33*, L23705, doi:10.1029/2006GL027185.
- Qian, L., S. C. Solomon, and T. J. Kane (2009), Seasonal variation of thermospheric density and composition, *J. Geophys. Res.*, *114*, A01312, doi:10.1029/2008JA013643.
- Richards, P. G., J. A. Fennelly, and D. G. Torr (1994), EUVAC: A solar EUV flux model for aeronomic calculations, *J. Geophys. Res.*, *99*, 8981, doi:10.1029/94JA00518.
- Richmond, A. D., E. C. Ridley, and R. G. Roble (1992), A thermosphere/ionosphere general circulation model with coupled electro-dynamics, *Geophys. Res. Lett.*, *19*, 601, doi:10.1029/92GL00401.
- Rishbeth, H., and R. G. Roble (1992), Cooling of the upper atmosphere by enhanced greenhouse gases: Modeling of thermospheric and ionospheric effects, *Planet. Space Sci.*, *40*, 1011, doi:10.1016/0032-0633(92)90141-A.
- Roble, R. G., and R. E. Dickinson (1989), How will changes in carbon dioxide and methane modify the mean structure of the mesosphere and thermosphere?, *Geophys. Res. Lett.*, *16*, 1441, doi:10.1029/GL016i012p01441.
- Roble, R. G., E. C. Ridley, A. D. Richmond, and R. E. Dickinson (1988), A coupled thermosphere/ionosphere general circulation model, *Geophys. Res. Lett.*, *15*, 1325, doi:10.1029/GL015i012p01325.
- Solomon, S. C., and L. Qian (2005), Solar extreme-ultraviolet irradiance for general circulation models, *J. Geophys. Res.*, *110*, A10306, doi:10.1029/2005JA011160.
- Woods, T. N., G. J. Rottman, S. M. Bailey, S. C. Solomon, and J. Worden (1998), Solar extreme ultraviolet irradiance measurements during solar cycle 22, *Sol. Phys.*, *177*, 133, doi:10.1023/A:1004912310883.
- Woods, T. N., F. G. Eparvier, S. M. Bailey, P. C. Chamberlin, J. Lean, G. J. Rottman, S. C. Solomon, W. K. Tobiska, and D. L. Woodraska (2005), Solar EUV Experiment (SEE): Mission overview and first results, *J. Geophys. Res.*, *110*, A01312, doi:10.1029/2004JA010765.
- Woods, T. N., P. C. Chamberlin, J. Harder, R. A. Hock, M. Snow, F. G. Eparvier, J. Fontenla, W. E. McClintock, and E. C. Richard (2009), Solar Irradiance Reference Spectra (SIRS) for the 2008 Whole Heliosphere Interval (WHI), *Geophys. Res. Lett.*, *36*, L01101, doi:10.1029/2008GL036373.

L. V. Didkovsky, Space Sciences Center, University of Southern California, SHS 274, Los Angeles, CA 90089, USA.

J. T. Emmert, Space Science Division, Naval Research Laboratory, Code 7643, 4555 Overlook Ave. SW, Washington, DC 20375, USA.

L. Qian and S. C. Solomon, High Altitude Observatory, National Center for Atmospheric Research, 1850 Table Mesa Dr., Boulder, CO 80307, USA. (stans@ucar.edu)

T. N. Woods, Laboratory for Atmospheric and Space Physics, University of Colorado at Boulder, 1234 Innovation Dr., Boulder, CO 80303, USA.